

EFFICIENT DETECTION OF PRODUCTION DEFECTS IN A CFRP AIRCRAFT COMPONENT BY MEANS OF FLASH INFRARED THERMOGRAPHY

Gaétan Poelman^{1,*}, Saeid Hedayatrasa^{1,2}, Joost Segers¹, Wim Van Paepegem¹ and Mathias Kersemans¹

¹ Department of Materials, Textiles and Chemical Engineering (MaTCh), Ghent University, Technologiepark-Zwijnaarde 46, 9052 Zwijnaarde, Belgium

² SIM Program M3 DETECT-IV, Technologiepark-Zwijnaarde 48, B-9052 Zwijnaarde, Belgium

* Corresponding author: Gaetan.Poelman@UGent.be

ABSTRACT

Flash thermography is a promising technique to perform quick and non-contact non-destructive testing of composite materials. However, several limitations such as non-uniform heating and lateral heat diffusion complicate the accurateness of this technique. This paper presents an experimental case study of flash thermography for the non-destructive testing of a CFRP component of an aircraft with production defects. Three post-processing techniques, namely Differential Absolute Contrast (DAC), Pulsed Phase Thermography (PPT) and Principal Component Thermography (PCT), are applied to the recorded dataset. A qualitative comparison between these processing techniques is performed based on their defect enhancement capabilities in a component with industrial complexity.

Keywords: Composites, NDT, Flash thermography, Post-processing techniques

1 INTRODUCTION

Fiber reinforced polymers are composite materials that have interesting properties such as a high specific stiffness and a good resistance against corrosion. Especially the fact that these materials are lightweight makes them attractive to the transportation industry (e.g. aerospace) by reducing both the fuel consumption and the carbon footprint. However, their layered structure makes them susceptible to damage features that may arise either during production or during in-service loading, and could eventually lead to failure of the part or the entire structure. It is thus critical to inspect a component in a non-destructive fashion in order to assess its structural integrity.

The ultrasonic C-scan technique is the current standard for non-destructive testing (NDT) in the industrial environment, however, it has several limitations: (i) requires a coupling liquid, (ii) is a slow NDT technique (scanning motion), (iii) has difficulties with the inspection of complex geometries (e.g. curved samples), and (iv) is not effective when dealing with very thin samples [1]. Flash thermography (FT) is a more recent but promising NDT technique that exploits the contrast in thermal properties between a defect and the sound area [2, 3]. In this technique, an optical source is used to rapidly heat up a sample's surface, after which the excited surface's cooling down regime is monitored with a high-end infrared (IR) camera. The induced through-thickness thermal gradient causes thermal waves to penetrate into the specimen, where the thermal conductivity mismatch between an internal boundary and the

sound area causes them to be reflected back to the excited surface. As such, a localized heat gradient is observed above the defected region, making it possible to detect local anomalies. This technique thus provides a (i) quick, (ii) full-field and (iii) contactless inspection of the sample [2]. However, considering that thermal waves are diffusive and highly damped in nature, the inspection of anisotropic composite materials and the detection of small and deep defects is very challenging.

In order to increase a defect's contrast with its surrounding area, while at the same time reducing unfavorable effects such as non-uniform heating, many data processing techniques have been developed in recent years. References [4-6] give an overview of most of these post-processing techniques. In this contribution, the focus lies on Differential Absolute Contrast (DAC) [7, 8], Pulsed Phase Thermography (PPT) [9, 10] and Principal Component Thermography (PCT) [11, 12]. A case study into their respective defect detectability enhancement is performed on a stiffened CFRP panel from the back tail of an Airbus A320 with real production defects. The paper is organized as follows: section 2 presents the used experimental procedure and the inspected material. Section 3 discusses the raw thermograms measured after flash excitation whereas the post-processed results are discussed in section 4. Finally, the main conclusions are gathered in section 5.

2 EXPERIMENTAL SETUP AND MATERIAL

A Hensel linear flash lamp was used as optical excitation source, consuming 6 kJ of energy to provide a 5 ms flash. The lamp was placed at a distance of 40 cm from the inspected component. The surface's temperature evolution was recorded with a high-end IR camera (FLIR A6750sc), placed 90 cm away from the sample. This camera has an array of 640×512 cryo-cooled InSb detectors with a noise equivalent differential temperature (NEDT) of < 20 mK, a bit depth of 14 bit and is sensitive in the $3\text{-}5 \mu\text{m}$ range. The camera was calibrated in the temperature range of $10\text{-}90$ °C. The synchronization of excitation and recording was guaranteed through soft- and hardware from edevis GmbH. A total duration of 50 s, which existed of 0.1 s pre-flash and 49.9 s of the cooling down regime after flash excitation, was recorded at a 50 Hz sampling frequency. Thus, a dataset of 2500 frames was obtained, which was 1.6 GB in data size. Figure 1(a) schematically illustrates the experimental set-up, and Figure 1(b) presents the typical temperature profile of a flash thermographic experiment (the non-hatched area is considered for data processing).

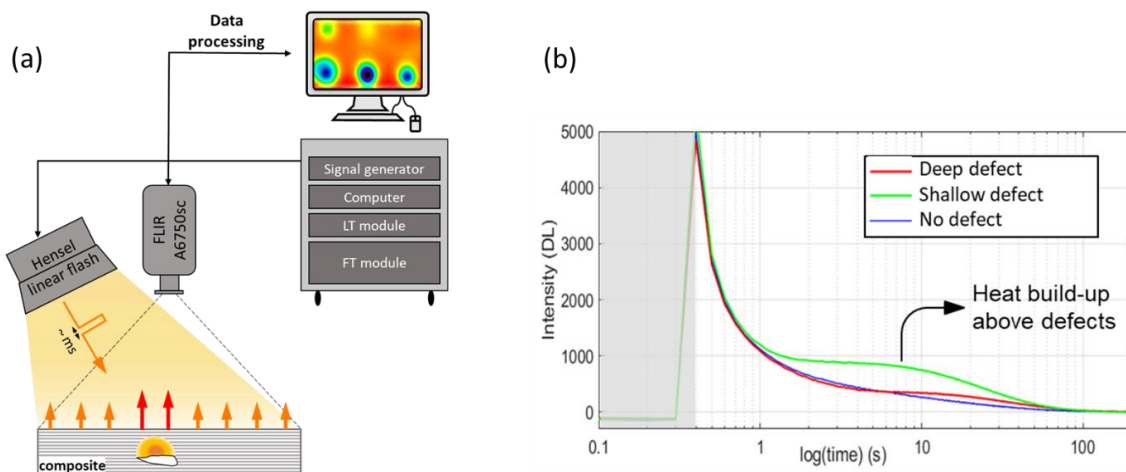


Figure 1: (a) Schematic illustration of the experimental procedure in flash thermography; (b) temperature profiles for a flash thermographic experiment.

For this case study, a part of a vertical tail of an Airbus A320 is investigated. The carbon fiber reinforced polymer (CFRP) component has a length of 610 mm, a maximum width of 200 mm at the left end, and has three stiffeners attached at the back side. The part was scrapped due to internal defects that were accidentally introduced during the production cycle. Images of the front and back side of the component are provided in Figure 2(a-b). A detailed C-scan was performed by the company SABCA Limburg, which is presented in Figure 2(c). Three peculiarities are identified:

- (1) Shallow delamination
- (2) Local disbond between the stiffener and the base plate
- (3) Back side label

First, the component's front side was sprayed with matt black paint so that all white surface markings were removed, after which the area highlighted as 'Region of interest' in Figure 2 was inspected with flash thermography.

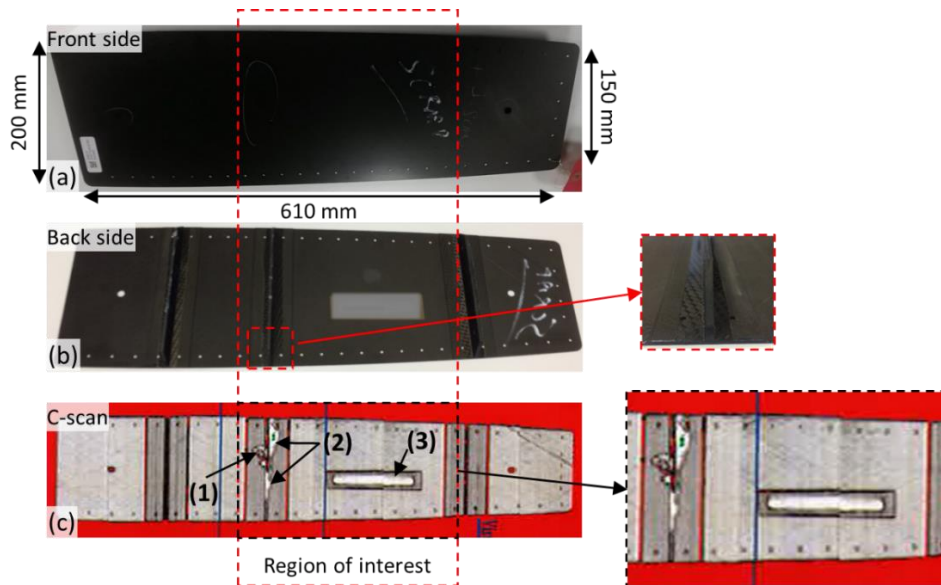


Figure 2: Scrapped part from a vertical tail of an Airbus A320. (a) view from the front side; (b) view from the back side with a side view of the stiffener) and (c) C-scan from SABCA Limburg.

3 UNPROCESSED RESULTS

After flash excitation, the excited surface's temperature follows an exponential decay (see Figure 1(b)). Four unprocessed thermograms are selected, which are presented in Figure 3. As expected when exciting with only one flash lamp, a significant amount of non-uniform heating is introduced, which in this case has its highest intensity at the top right side. At 0.4 s after the flash excitation (Figure 3(a)), the delaminated area is already visible, indicating that this internal defect is located very near to the excited surface (i.e. shallow defect). The other defects remain undetected in this thermogram. In a later frame at 0.7 s (Figure 3(b)), the stiffeners and label at the back side start to become apparent. The local thickness increase at these locations causes the surface to cool down more rapidly than the surrounding thinner material. At 0.9 s (Figure 3(c)), a local disturbance of the delaminated area at the left stiffener can be observed, however, the indication is blurry. Also, the stiffeners and the back side label are now more clearly observed in the raw thermogram. Notice that the back side label only causes a detectable disturbance for the upper half. The contrast of the delaminated area decreases since the heat accumulated on top of the defect is redistributed through lateral heat diffusion. In the last

selected thermogram at 1.5 s (Figure 3(d)), the contrast of the stiffeners and the back side label at the back side is further increased while the detectability of the delamination has reduced further. The debonded area still only provides a blurry indication.

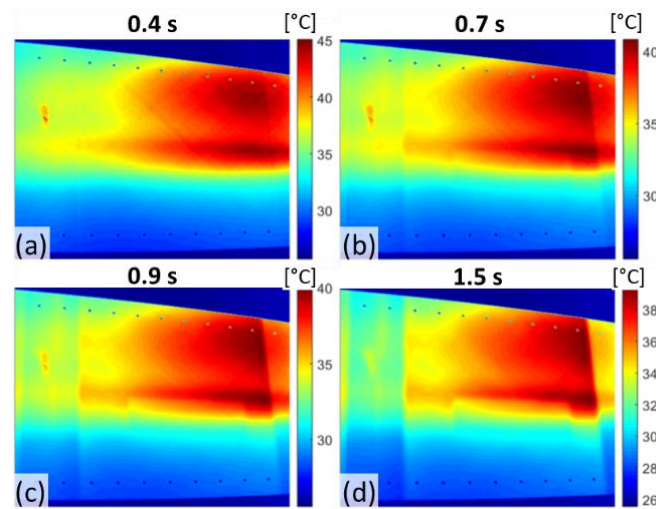


Figure 3: Unprocessed thermograms at (a) 0.4 s; (b) 0.7 s; (c) 0.9 s and (d) 1.5 s after flash excitation.

In the raw thermograms, all features of the inspected component (i.e. delamination, debonding, back side label and stiffeners) can be perceived if you have prior knowledge on what to expect. Even with this foreknowledge, it is difficult to pinpoint the debonding and the back side label due to a low mismatch in thermal conductivity with the surrounding sound material and the non-uniform heating. In order to better extract damage features, data processing must be performed.

4 RESULTS AFTER POST-PROCESSING

Before applying post-processing techniques, it is common practice in flash thermography to first perform cold image subtraction to reduce effects of background reflections and non-uniform surface properties. Saturated frames are also removed from the sequence. The post-processing techniques that were applied on this pre-processed dataset are discussed below.

4.1 Differential absolute contrast (DAC)

The first post-processing technique for flash thermographic data is called Differential Absolute Contrast (DAC). This method is based on the notion that it takes some time for a defect to manifest itself in the recorded sequence due to the travelling time of the induced thermal waves inside the specimen [7]. Before any defect becomes visible, a sound and a defected pixel thus behave similar. This makes it possible to compute the behavior of a sound pixel over time by considering the 1D analytical solution of FT, which means that no reference pixel needs to be selected. The output of the DAC is then obtained by subtracting the measured temperature profile from the estimated sound behavior. Generally speaking, this technique provides good results for thin samples and for early time frames [7]. The application of DAC to all 2500 frames on a laptop with an Intel Core i7 CPU and 32 GB of RAM took around 5 s. Since a contrast map is calculated for each time frame, no data compression is performed.

The output of the DAC at the same time instances as the unprocessed data is presented in Figure 4. It is immediately clear that the disturbing non-uniform heating pattern is significantly

reduced by DAC in all considered time frames. At 0.4 s (Figure 4(a)), the delamination exhibits a much better contrast than in the raw thermogram (Figure 3(a)). While the stiffeners and the back side label at the back side were only faintly observable in the raw data at 0.7 s (Figure 3(b)), the application of DAC renders their detection much more straightforward. Moreover, the bottom edge of the back side label can now also be identified. At later times (Figure 4(c-d)), the presence of the debonding of the stiffener is clearly detectable, marking a huge improvement over the raw input. A clear indication of the label at the back side is also obtained in these images.

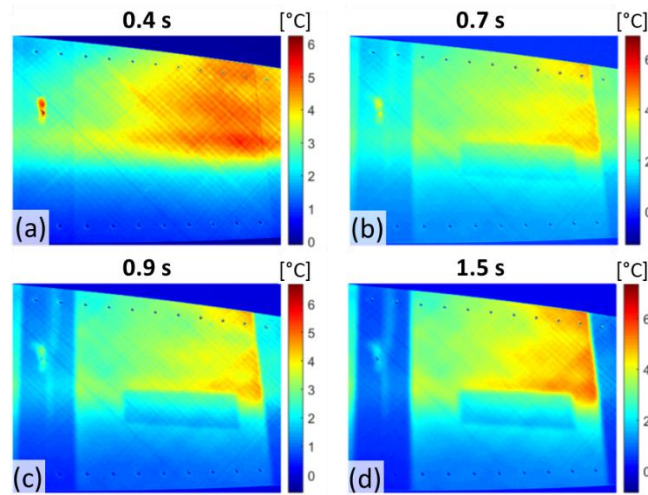


Figure 4: Frames after applying DAC at (a) 0.4 s; (b) 0.7 s; (c) 0.9 s and (d) 1.5 s after flash excitation.

4.2 Pulsed phase thermography (PPT)

In Pulsed Phase Thermography (PPT), the recorded signal for each pixel is decomposed into its harmonic components through the fast Fourier transform (FFT) [9, 10]. Since a short pulse in time domain corresponds to a wide range of frequencies in frequency domain, thermal waves of many different frequencies are excited by the optical flash. Furthermore, the thermal diffusion length of a thermal wave is inversely proportional to its frequency, meaning that lowering the evaluation frequency provides a deeper probing into the material. In the general case, amplitude and phase maps are obtained by performing FFT. However, since the phase is emissivity-normalized (suppression of non-uniform heating, background reflections and non-uniform surface properties), this quantity is typically used. With this technique, a data size reduction of 50% is obtained (resulting in 0.8 GB). The calculation of the resulting phase maps required 21 s.

In Figure 5(a), the resulting phase map at 1 Hz is presented. In this image, the delamination in the left stiffener is very clearly observed, as are the stiffeners themselves. Notice also that an imprint is obtained of the dominant fiber orientation ($\pm 45^\circ$). Furthermore, the bottom half of the sample, where the amount of deposited excitation energy was lower, is more noisy than the upper half. By lowering the frequency to 0.5 Hz (Figure 5(b)), the delamination loses phase contrast. The detectability of the debonded area becomes very high when the frequency is further reduced to 0.2 Hz. At this frequency, the back side label is also straightforward to observe. In this image, there are some non-uniformities in the area between both stiffeners, which means that care should be taken when only evaluating one specific frequency. At the even lower frequency of 0.1 Hz (Figure 5(d)), the edges of the defects lose their sharpness,

which is an indicator that this evaluation frequency is too low. Finally, instead of evaluating each frequency separately, it is also possible to combine several frequencies so that only one image needs to be assessed. This is done in Figure 5(e), where all frequency bins from 0.1 Hz up to 1 Hz are combined by a pixel-wise summation after frame-wise mean-value subtraction. In this combined image, the shallow delamination and the back side label are both clearly observable. However, the debonding is not clearly extractable. This illustrates that the selection of the optimal frequency range for the combination is not straightforward and deserves further investigation.

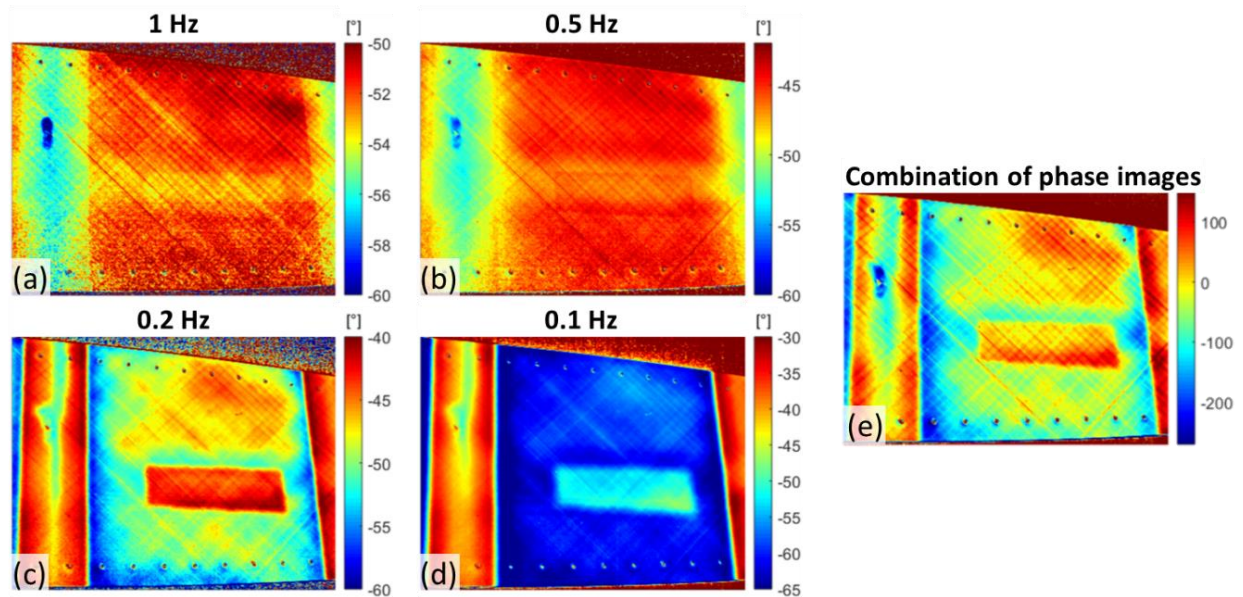


Figure 5: (a-d) phase images at 1 Hz, 0.5 Hz, 0.2 Hz and 0.1 Hz, respectively; (e) image obtained after combination of the phase images from 1 Hz to 0.1 Hz.

4.3 Principal component thermography (PCT)

The final processing technique that is discussed in this paper is Principal Component Thermography (PCT), in which the recorded signal is not projected upon a prescribed set of orthogonal functions (e.g. the FFT uses oscillatory functions) [11, 12]. Instead, the singular value decomposition of an appropriately organized matrix constructs a set of orthogonal statistical modes that provide the strongest projection for the input data. For a flash thermographic dataset, the first few principal components (PC) typically explain almost all the input's variability, thus providing a very significant data compression (e.g. 2500 frames compressed into 10 PCs). The time required to calculate the first 10 PCs was 107 s, which makes this the most computationally expensive technique of the ones discussed in this contribution.

The four principal components that provide most information for defect detection are presented in Figure 6(a-d). In the second PC (Figure 6(a)), the stiffeners are clearly observed, and some local distortion can be perceived at the location of the delamination. Also, the back side label is straightforward to extract from this image. In PC 3 (Figure 6(b)), the detection of the delamination is enhanced in comparison to PC 2. The best detection of the debonded area is found in PC 4 (Figure 6(c)), while the back side label and the delamination are also observable in this image. In PC 5 (Figure 6(d)), only the upper region of the debonding and the delamination are detectable. In general, it is far from straightforward to select one optimal

principal component image to evaluate as it is not yet fully understood which principal component corresponds to which features. For this reason, a combination of the first 10 PC images is presented in Figure 6(e). In this image, all three defect features are easily found, however, due to the combination, information with respect to depth is lost in this image. As was the case with PPT, the selection of the images to be used in the combination here is also not straightforward. To truly exploit the available information to the fullest, this would need to be investigated.

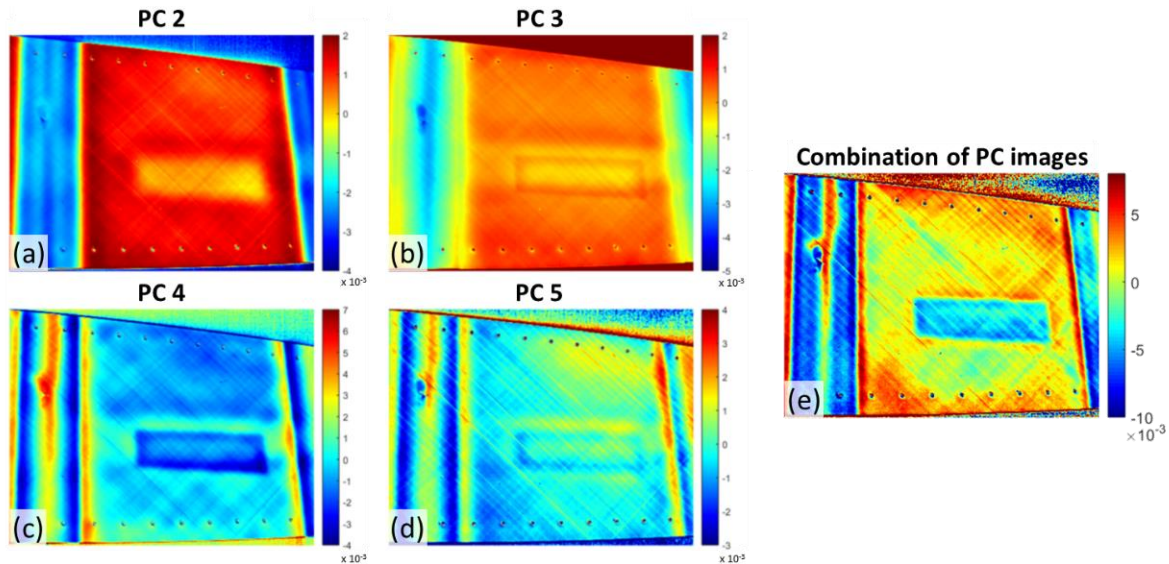


Figure 6: (a-d) PC images 2 through 5; (e) image obtained after combination of first 10 PCs.

5 CONCLUSIONS

A scrapped sample from an Airbus A320 with backside stiffeners and multiple complex damage features (shallow delamination, debonding below the stiffener and a back side label) was investigated through flash thermography. The recorded thermographic sequence was evaluated and post-processed by means of three data analysis techniques, namely differential absolute contrast (DAC), pulsed phase thermography (PPT) and principal component thermography (PCT).

The unprocessed data from the flash thermographic experiment was sufficient to detect the shallow delamination, however, only blurry indications of the debonded area and the back side label were obtained. Without foreknowledge on the part and its defects, correct defect identification would be almost impossible. The application of DAC significantly improved the detection of the debonded area, while also increasing the detectability of the other damage features. This technique was further outperformed by the PPT, which showed the best defect enhancement at an evaluation frequency of 0.2 Hz. A combination of several evaluation frequencies into one image improved the overall defect detection, but can complicate the defect sizing. Lastly, a combination of several PCs was the best technique for detecting the different defect features, but is more difficult to interpret than DAC and PPT. Overall, it is a trade-off between calculation time and defect enhancement.

ACKNOWLEDGEMENTS

The authors acknowledge the SBO project DETECT-IV (Grant no. 160455), which fits in the SIM research program MacroModelMat (M3) coordinated by Siemens (Siemens Digital Industries Software, Belgium) and funded by SIM (Strategic Initiative Materials in Flanders)

and VLAIO (Flemish government agency Flanders Innovation & Entrepreneurship). The authors further acknowledge Fonds voor Wetenschappelijk Onderzoek Vlaanderen (FWO-Vlaanderen) through grants 1S11520N, 1148018N and 12T5418N. SABCA Limburg is acknowledged for providing the test specimen, together with its C-scan.

REFERENCES

- [1] Scott, I.G. and C.M. Scala, *A review of non-destructive testing of composite materials*. NDT International, 1982. **15**: p. 75-86.
- [2] Yang, R. and Y. He, *Optically and non-optically excited thermography for composites: A review*. Infrared Physics & Technology, 2016. **75**: p. 26-50.
- [3] Milne, J.M. and W.N. Reynolds, *The non-destructive evaluation of composites and other materials by thermal pulse video thermography*. Thermosense VII, 1985: p. 119-1222.
- [4] Ciampa, F., et al., *Recent Advances in Active Infrared Thermography for Non-Destructive Testing of Aerospace Components*. Sensors (Basel), 2018. **18**(2).
- [5] Vavilov, V.P. and D.D. Burleigh, *Review of pulsed thermal NDT: Physical principles, theory and data processing*. NDT & E International, 2015. **73**: p. 28-52.
- [6] Ibarra-Castanedo, C., et al., *On signal transforms applied to pulsed thermography*. Recent Res. Devel. Applied Phys., 2006. **9**.
- [7] Pilla, M., et al. *New Absolute Contrast for pulsed thermography*. in *Proceedings of the 2002 International Conference on Quantitative InfraRed Thermography*. 2002.
- [8] Benítez, H.D., et al., *Definition of a new thermal contrast and pulse correction for defect quantification in pulsed thermography*. Infrared Physics & Technology, 2008. **51**(3): p. 160-167.
- [9] Maldague, X. and S. Marinetti, *Pulse phase infrared thermography*. Journal of Applied Physics, 1996. **79**(5): p. 2694-2698.
- [10] Oswald-Tranta, B., *Time and frequency behaviour in TSR and PPT evaluation for flash thermography*. Quantitative InfraRed Thermography Journal, 2017. **14**(2): p. 164-184.
- [11] Rajic, N. and DSTO-TR-1298, *Principal Component Thermography*. 2002, Defence Science and Technology Organisation Victoria (Australia) Aeronautical and Maritime Research Lab. p. 38.
- [12] Rajic, N., *Principal component thermography for flaw contrast enhancement and flaw depth characterisation in composite structures*. Composite Structures, 2002. **58**(4): p. 521-528.